F Colao et al.

LIBS experiments for quantitative detection of retained fuel

Preprint of Paper to be submitted for publication in
22nd International Conference on Plasma Surface Interactions
in Controlled Fusion Devices (22nd PSI)

LIBS experiments for quantitative detection of retained fuel

F. Colao(*), S. Almaviva, L. Caneve, G. Maddaluno, T. Fornal[a],
P. Gasior[a], M. Kubkowska[a] , M. Rosinski[a]

ENEA, Italian National Agency for New Technologies, Energy and sustainable Economic Development, C.R. Frascati, via Enrico Fermi, 44, 00045 – Frascati (Italy)
[a] *IPPLM, Institute of Plasma Physics and Laser Microfusion, 00-908 Warsaw, P.O. Box 49, Hery St. 23, Poland*
(*) corresponding author: francesco.colao@enea.it

Abstract

Laser Induced Breakdown Spectroscopy (LIBS) provides chemical information from atomic and ionic plasma emissions generated by laser vaporization of a sample. At the ENEA research center, in collaboration with IPPLM, an equipment has been set up to qualitatively and quantitatively determine the chemical composition of impurities deposited on Plasma Facing Components (PFC). The strength of the LIBS, for its capability of light elements detection, is fully exploited to determine the deuterium content since this element can be considered as the best choice proxy for tritium; the latter being is of great importance in assessing safe conditions to assure the continuous operation in nuclear fusion tokamak.

Here we present the results of the Double Pulse LIBS (DP-LIBS) probing of deuterated samples with the simultaneous optical detection by medium-resolution and high-resolution spectrometer. Deuterium emission at 656.1nm has been detected then the elemental composition has been quantified by applying the Calibration Free (CF) approach. The obtained results demonstrate that the DPLIBS technique combined with CF analysis is suitable for the quantitative determination of tritium content inside the PFCs of next fusion devices like ITER.

Introduction

The process of laser ablation of metals is complex; it in fact depends on several factors including the material, the environmental parameters and the laser pulse excitation in terms of pulse energy, time duration, wavelength, and beam quality [1,2]. In order to obtain satisfactory quantitative analysis, especially in case of determination of trace elements, it is necessary a good understanding of the interaction of the sample with the laser [3]; also the phenomena associated with the laser ablation must be carefully considered since the signal is proportional to the density of the emitting species and definitively to the ablated mass.

LIBS studies in vacuum [4, 5] have shown that the multiphoton ionization provides the initial electrons and plays a very important role for the breakdown phenomenon; here the electron free path well exceed the plasma volume and the electron cascade is strongly depressed. The double pulse LIBS plays in vacuum a crucial role; indeed provided that the interpulse delay is of the order of magnitude of the ratio between the plasma mean radius and the particles velocity, the first pulse substantially modifies the local density of particles facing the second laser pulse favoring the laser plasma interactions and increasing the abated mass [6].

The typical laboratory plasmas are characterized by a predominance of the electron impact processes, while the radiative losses do have a negligible contribution to the plasma kinetics [7]. Moreover the possibility to define a suitable time window for the existence of a Local Thermodynamic Equilibrium (LTE) is currently accepted. Accordingly it is possible to define a

local temperature T at each point in space in such a way that the plasma formed by atoms, ions and electrons, is uniquely described by means of the number density of electrons and one thermodynamic parameter, namely the temperature which is assumed to be the same for all the species present in the plasma [8]. In LTE, the species density follows the Saha-Eggert relationship, while the ions and electrons energy distribution are described by Boltzmann and Maxwell respectively [8]. It is therefore possible to analytically model the atoms and ions populations, nevertheless their exact computation critically depend on the partition function, which requires the availability of a sufficiently complete set of atomic energy levels as well as an appropriate definition of the ionization potential lowering [9].

The quantitative determination of tritium content inside the PFCs of next fusion devices like ITER, mandatory both for safety reason, is best accomplished by in situ real time technique; LIBS is one of the most promising, however the assessment of the attained accuracy must be assessed [10].

Several conditions must be fulfilled when using the LIBS spectrometry for quantitative analytical applications, whose main objective is to provide quantitative information with high accuracy and precision. In this case it is required that the ablated material has a composition similar to that of the sample under analysis; a simplifying condition is also obtained whenever the plasma is optically thin, since in this case the effect of self-absorption of the radiation emitted from the plasma itself is avoided [11]. The concentration of sample elemental constituents can be obtained by means of the calibration curve, i.e. a relationship between the response and the mass or concentration of the analyte in a given range. Quantitative analysis by means of calibration curves presents several drawbacks mainly related to the effect matrix [12]; in order to reduce the influence of the matrix, reference samples must be made with a composition similar to that of the unknown sample. On the other hand the technique requires the availability of reference samples with a wide range of concentration, encompassing that of the analyte in question. Finally a calibration curve is needed for each one of the elements under study. It is possible to overcome these problems by using standard-less calibration methods with special reference to the Calibration Free (CF) technique; moreover it is worth mention that the approaches devised for the quantitative determination of the minor constituents lead to accuracy of the order of 20%, which is well within the requirement put by fusion machines as for example ITER.

Experimental

The sample used for this work was prepared by coating a molybdenum substrate with a 1.5 μ thick tungsten layer. Successively the sample was exposed to D_2 plasma in the Pilot-PSI device [13]. The plasma flow was about 16.9 mbar l s^{-1}, corresponding to 4.1 10^{20} ions s^{-1}, the FWHM of the beam about 25 mm and the exposure time 910 s, on an implanted area of about 5 cm^2. The surface density of impinging ions was 7.6 10^{26} ions/m^2 .The energy of the D ions was determined by the sample biasing and was 40 eV; the sample temperature during the implantation was between 200 C and 300 C.

The main components of the used LIBS set up are shown in Figure 1. Basic components of the experimental set-up are a twin laser, a focusing lens and a detection system to spectrally resolve the collected light; finally a personal computer is used for signal processing and data storage.
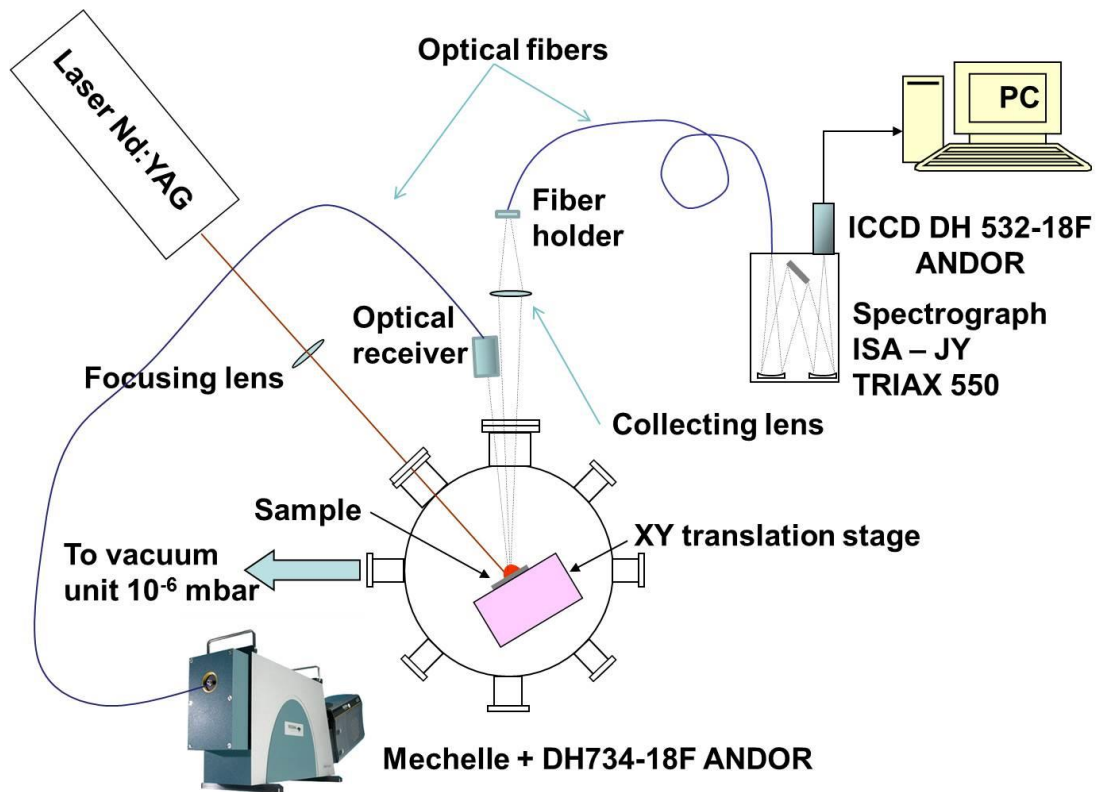
Figure 1 – LIBS setup

The excitation source is a solid state laser system (TII LS-2131D from LOTIS LOT); the flash lamps independently pump two Nd:YAG rods each of them is capable to produce typical pulse widths of 9-12 ns at the fundamental wavelength at 1064 nm. Two Q-switched independent resonators leave the user with a complete freedom for selecting the interpulse delay and pulse energy in the range from 50mJ to 200mJ. The laser pulse repetition rate is 10Hz, and a single 500mm planoconvex BK-7 lens is used to focus the laser beam to ablate the sample.

High and low spectral resolution is simultaneously achieved by two different optical assemblies; the first is a condenser-fiber assembly allowing for narrow band high resolution, while the second condenser-fiber assembly is used for broadband low resolution measurements.

In lens-fiber configuration, a single 150 mm focal length planoconvex lens is coupled into a circular bundle end of 22 individual fibers. The lens is positioned at 30cm from both sample and fiber bundle end for an optimized light collection. The other end of the fiber bundle is configured as linear array and is placed in front of the entrance slit of the spectrometer (50um). The collected light is focused into a 0.55 meter focal length CzernyTurner spectrograph (Triax 550, Yobin-Ivone) spectrally dispersed by a 2400 grooves/mm grating with a spectral resolution of $\delta\lambda/\lambda = 15000$. The detector is an ICCD camera (DH534-18F, Andor) with 1024x256 pixel array and covers a spectral window of 12 nm.

In condenser-fiber assembly, the optical receiver (ME-OPT-007, Andor) is placed at 35cm from the sample; the exit of the condenser is coupled into a 50um fiber. The other end of the

fiber is connected to the entrance port of the spectrometer. The collected light is focused into a echelle (Mechelle 5000, Andor) detected by an ICCD camera (DH734-18F, Andor).

This arrangement provides both the possibility of well resolving the hydrogen and its isotopes, while allowing for a better estimate of plasma parameters from the many available lines emitted from sample major constituents and spanning over the spacrtal range form 250 to 800nm.

The chamber containing the sample under study is connected to a vacuum system (Turbolab, Leybold); the pressure inside the analysis chamber is 10^{-5} mbar. The sample holder is mounted on a XY translator stage, so that unexposed sample surface can be faced to the ablating laser.

Result and discussion

The Double Pulse (DP) technique has been reported as a viable technique to enhance the LIBS signal in several experimental conditions including the atmospheric air pressure [14] and vacuum [15]. The mechanisms responsible of the signal enhancement are mainly related to the modifications in the environment produced by the first laser pulse, which create the optimal conditions for the laser target and laser plume interactions of the second laser pulse. Babushok et al. in [14] discuss various parameters which characterize both the processes in the target material and in the gas plasma plume. Mechanisms responsible for enhancement in nanosecond excitation DPLIBS at atmospheric pressure are related to the changes in the environment surrounding the sample caused by the first laser pulse; consequently the second laser pulse undergoes to lower shielding and a better coupling with the target. On the other hand in DPLIBS in vacuum the plasma induced by the first laser pulse expands almost freely in the absence of counterpressure of the ambient gas, with low density low plasma absorption, while the second laser pulse is effectively coupled with plasma.

In current experiment vacuum at residual pressure of 10-5mbar was used; a careful optimization of the experimental parameters (interpulse delay gate duration and delay) allowed optimum compromise between ablated mass and plasma temperature.

Individual DPLIBS spectra were simultaneously acquired for the same laser shot by two acquisition systems. Interpulse delay plays an important role in DPLIBS signal enhancement sine it regulates the laser interactions with the target and the plasma, thus influencing the ablation efficiency and plasma re-heating processes. For this experiment the delay between the two lasers was optimized to 300ns. The laser pulse energy we used was 200 mJ ∕ pulse for first pulse (1064 nm) and 200 mJ ∕ pulse for second pulse (1064 nm), and this also shows an optimum value. A typical single-shot, low resolution LIBS spectrum for laser shot #32 is shown in figure 2 in the spectral windows is from 200 to 900nm, the delay between the excitation and detection was optimized 600 ns (see below), while the detection gate was 1200ns. For the same laser shot a corresponding high resolution spectrum was simultaneously acquired and it is shown in figure 3 for the 654nm to 659nm spectral region. The delay between the excitation and detection was 600ns as before, while the detection gate was 100ns.
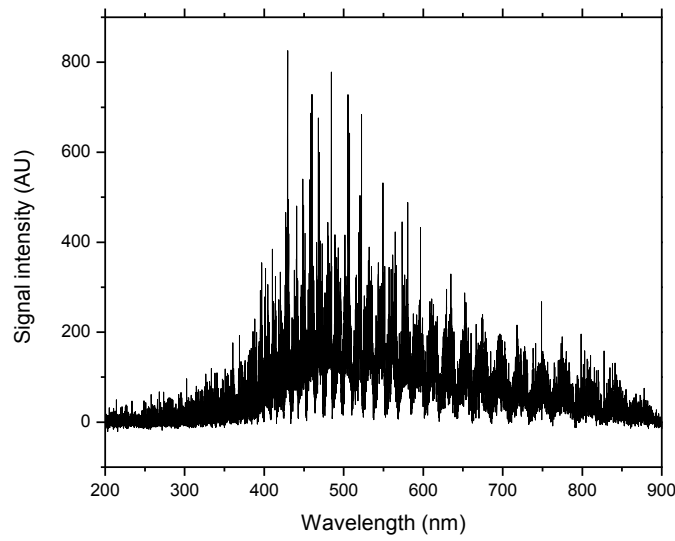
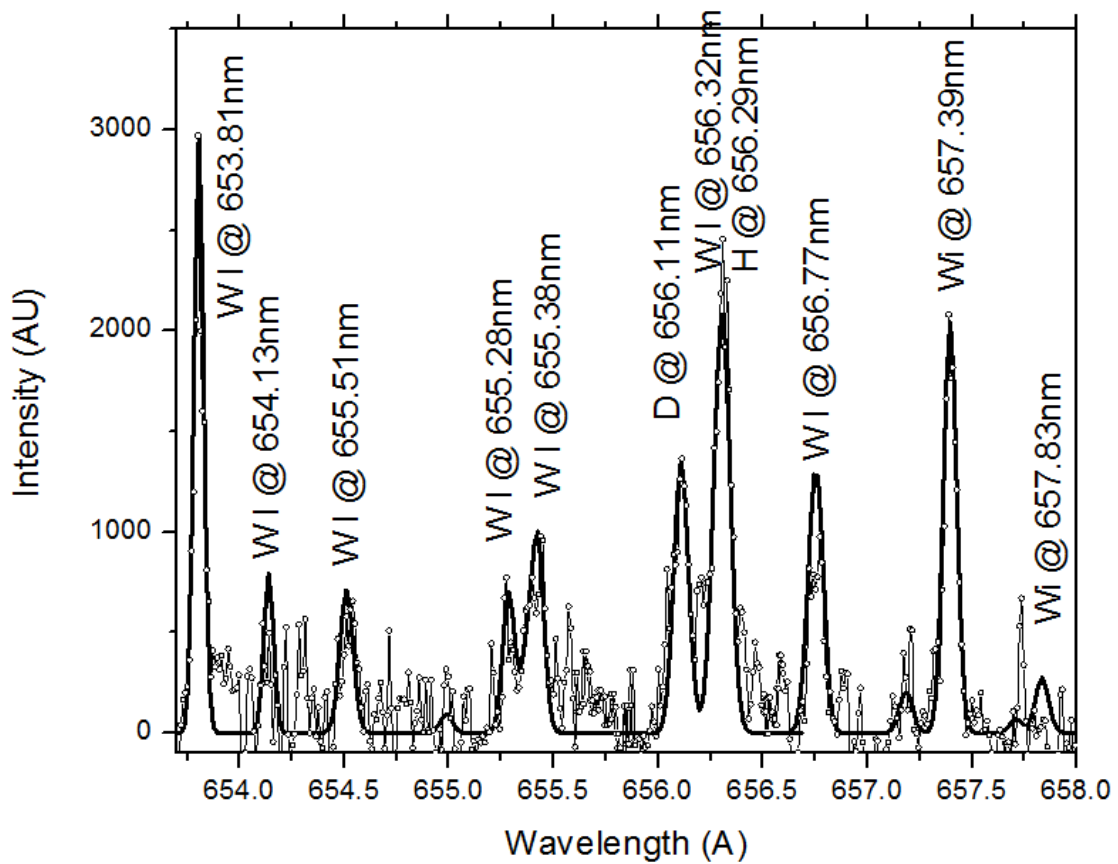Figure 2 –Low resolution LIBS spectrum on deuterated sample.

Figure 3 –High resolution LIBS spectrum on deuterated sample (dot experimental data, continuous line best fit)

Actual experimentation showed the simultaneous presence in the LIBS spectra of H and D lines, where the hydrogen contribution is due to contamination with sample exposure to the environment at atmospheric pressure. Previous study in a reduced atmosphere following the time dynamic of the relative contribution of H and D showed a segregation of the deuterium [16]. This effect, which is especially relevant in vacuum where the plume expansion is more pronounced, is consistent with a mass-dependent expansion dynamics and for double pulse experiment suggests the use of relatively large gate delay to enhance the sensitivity and favour the analytical determination of deuterium. Optimization of the detection of Da line (see figure f) was obtained in this study using a gate delay of 600ns and gate with of only 100ns; use of narrow gate with also facilitate the stationarity of the detected emission., reducing problems connected with Ne and Te time dependence.

Plasma temperature (Te) was determined using the Boltzmann plot and assuming LTE conditions. Each LIBS spectrum is obtained from a single laser shot and the experimental line intensity corrected for the spectral efficiency was plotted against the energy of upper level for each transition. Figure 4 shows the Boltzmann plot on laser shot 32 obtained on the examined sample; the selected analytical lines form a superset of the critical selection made by Lissovski [17].
The temperature is then calculated by using straight-line approximation fit to the data, where the slope of the line is equal to $-1/kT$.
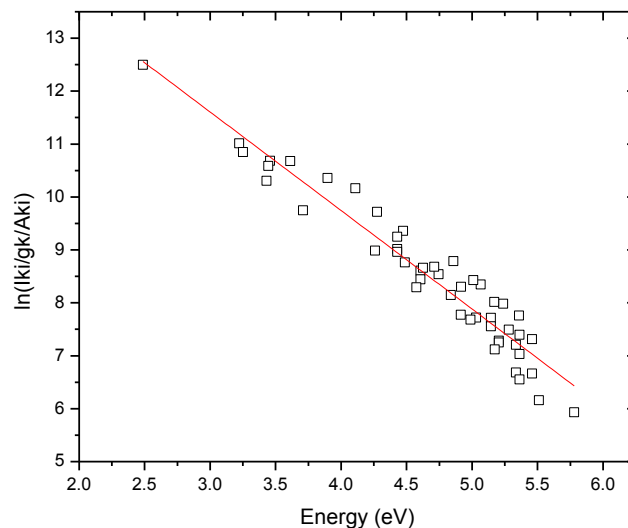

Figure 4 - Boltzmann plot of DP LIBS at gate delay of 600ns from the first laser pulse.

The electron density was derived from the analysis of Stark broadened spectral line profile of the D_α line at 656.1 nm. Use of that line has several significant practical advantages since it is optically thin and has a relatively large Lorentzian broadening, thus ensuring a small error in electron density computation.

The theoretical Stark broadening of the D_α line is obtained by modifying the approximation of Gigosos [18] to account for the fact that in the range of electron density between 10^{15} and 10^{17} cm^{-3} the experimental Stark broadening of Balmer alpha line of deuterium line is approximately 10% smaller than the corresponding line width of hydrogen [19]. The equation relating the electron density to the line full with at half area (FWHA) is obtained by using a modified version of the Gigosos broadening coefficient and reads as:

$$Ne = 10^{17} (\Delta\lambda_{FWHA} / 0.499)^{1.4713} \qquad (1)$$

where Ne is in cm^{-3} units and the $\Delta\lambda_{FWHA}$ is expressed in nm.

Line profile of D_α line was recorded with the high resolution Czerny-Turner spectrograph, then the experimental line profile was fitted with a Voigt curve; here the gaussian contribution accounts for the instrumental and the Doppler broadening, whereas the lorentzian contribution accounts for the natural and Stark broadening.

The instrumental broadening, evaluated from the low pressure glow discharge lamp (Ne I emission at 650.65 nm Oriel 6032), was found to be ~ 0.030 nm, while the Doppler broadening at T = 6500K, is evaluated to be ~ 0.032 nm. The overall gaussian broadening, estimated as the result of the convolution of instrumental and Doppler contributions, is given by [20]

$$FWHM_{gaussian} = \left(FWHM_{instr}^2 + FWHM_{Doppler}^2\right)^{1/2} = 0.044\text{nm} \qquad (3)$$

The gaussian broadening is then inserted as a constant parameter in the Voigt fitting function and the lorentzian contribution was computed by best fitting the theoretical profile with the experimental lineshape (see figure 5).
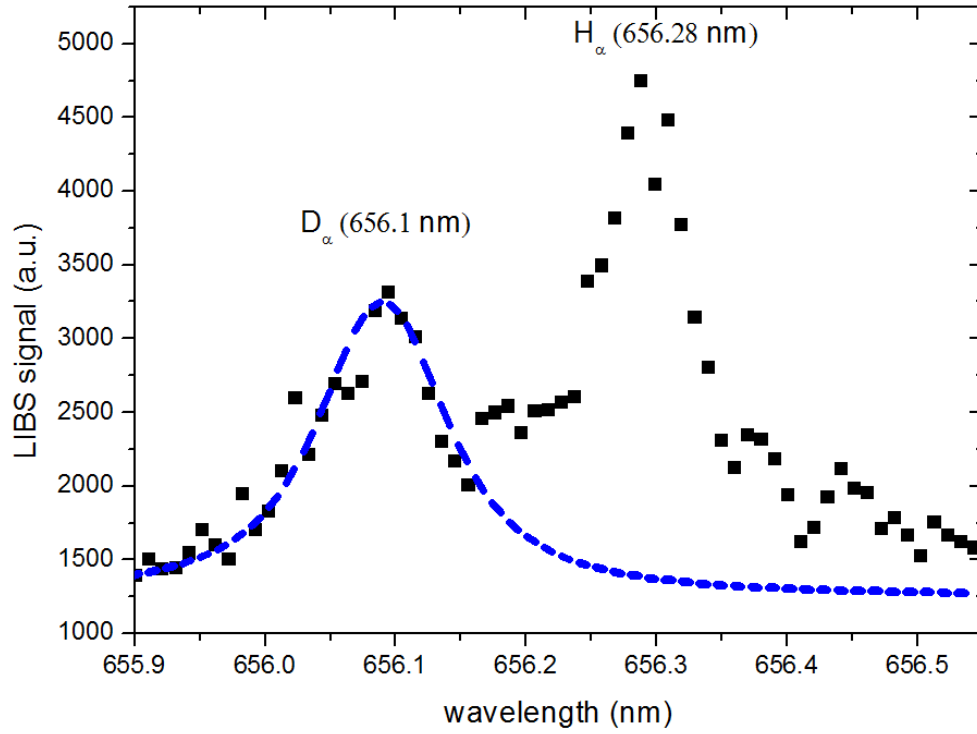
Figure 5 - Experimental data (square dot) and Voigt profile (continuous line) of the D_α emission at 656.1 nm.

The lorentzian broadening was about 0.13 ± 0.06 nm, while the density was Ne = (1.3 ± 0.6)10^{16} cm^{-3}. This value is numerically consistent with the electron density value obtained using the approximation accounting for ion and electron broadening computed by using the fractional intensity width of hydrogen tabulated by Griem [21].

The temperature and the electron density function of the gate delay are shown in Figure 6; for delay time ranging from 500 ns to 1000 ns the electron number density varied from 0.5 10^{16} to 1.3 10^{16} cm^{-3}.

A necessary condition for the LTE assumption is the McWirther criterion, giving the lower limit for the electron number density to maintain the energy level populations to within 10% of Boltzman equilibrium, while competing with radiative processes. Evaluation for the W I transition at 429.46 nm, ΔE=3 eV, and at the highest temperature in this study, the lower limit for Ne is 3.5 10^{15} cm^{-3}, which is lower than the value deduced from Stark broadening. Although the satisfaction of the McWirter criterion is not a sufficient condition, the existence of LTE is assumed in the following.
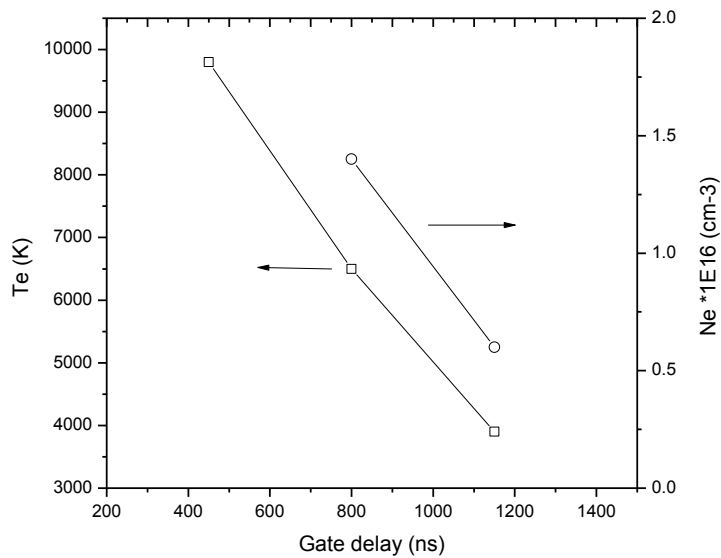
Figure 6 – Electron temperature (left scale) and density (right scale) for DPLIBS experiment versus gate delay computed from the first laser pulse.
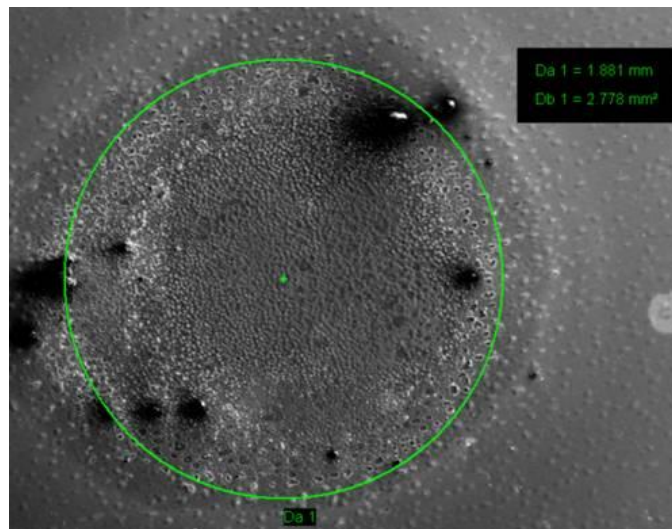

Figure 7 – SEM image of crater produced by DPLIBS; for this particular case one couple of laser pulses of 200+200 mJ each was used, with 300ns interpulse delay.

To estimate the power density delivered to the sample, superficial analysis by SEM is presented. The crater produced by a single laser shot in double pulse regime is presented in Figure 7. As can be seen the crater size has a circular shape; besides crater formation, thermal effects produce damage and melting fragment are visible on the border. Considering thermal effects as part of the superficial sample destruction, the irradiated area extends over a circular region of approximately 1800 μm of diameter. For this particular example the ablative pulses of $200 + 200$ mJ resulted in a power density of $1.8 GW/cm^2$; it must be noted however that the

laser energy effectively coupled with the target can be substantially less since the plasma generated from the first laser pulse effectively shields the second laser pulse. This mechanism strongly depends on the inter-pulse delay which dictates the laser interactions with the plasma and influences the ablation efficiency. Finally we observe that the measured power density is consistent with a stoichiometric ablation of the sample, thus satisfying a basic assumption of DPLIBS.

Application of the Calibration Free method to the sample under study gives a deuterium content concentration of (1.3 +/- 02) % at units. The D concentration can be compared with the one measured with Nuclear Reaction Analysis (NRA) on a tungsten sample implanted in Pilot-PSI with similar deuterium fluence [22]. In that experiment a polycrystalline tungsten target was implanted with 40 eV deuterium flux of $1.0 \ 10^{24} \ m^{-2}s^{-1}$ for 750 s, resulting in a fluence of $0.8 \ 10^{27} \ m^{-2}$. The concentration of D as measured by NRA was maximum at the near surface and equal to 1% at; taking into account the different kind of tungsten sample (tungsten bulk and tungsten coating on molybdenum substrate) the obtained result is in satisfactory agreement with LIBS measurements,

Based on previous estimates of the ablation efficiency, the mass removal is in the order of 20-40 μg. It is worth noticing that the assessment of the ablated material paves the way to a quantitative estimate of the total amount of deuterium contained in the sample, once the relative contribution of deuterium is known from the Calibration Free analysis.

Conclusions

The combination of DP-LIBS and Calibration Free analysis has been used for quantitative analysis of deuterium. Relatively high ablative energies densities produced limited thermal effect, and assured for stoichiometric ablation; the results obtained in the present experiments indicate the possibility to perform deuterium quantitative determination, and the same technique can also be applied for the quantification of tritium. The changes in the environment produced by double plasma excitation, demonstrate that the DP technique is an effective method for LIBS signal enhancement. In this case, the plasma produced by the second laser pulse together with the reheating of the plasma produced by the first laser, lead to an increase of density particles and of the collision rates which contribute to populate higher energy states in the atoms and consequently to an enhancement of the emission intensity.

Changing the surrounding environment of plasmas is a potential method for improving LIBS sensitivity which eventually can be combined with other enhancing effects such as magnetic field present in fusion machines without adding any design complexity.

The matrix effect and the problems related to the surface contaminants expected in fusion machines has overcome by using the Calibration Free technique; moreover it is worth mention that the approach here presented to determine the concentration of minor constituents shows an accuracy of the order of 20%, which is within the requirement put forward by fusion machines as for example ITER.

References

1. E. Tognoni, V. Palleschi, M. Corsi, G. Cristoforetti, Spectrochim. Acta Part B, 57, 1115, (2002).

2. R. E. Neuhauser, U. Panne and R. Niessner, Laser-induced plasma spectroscopy, Anal. Chem. Acta, 392, 47–54, (1999).

3. R. E. Russo, Appl. Spectrosc., 14A, 49, (1995).

4. A. Lissovskia, , 1, , K. Piipa, L. Hämarika, M. Aintsa, M. Laana, P. Parisa, A. Hakolab, J. Karhunenb, LIBS for tungsten diagnostics in vacuum: Selection of analytes, JNM, 463, 923–926, (2015).

5. W.Zhenzhen Wang Y.Deguchi J.Yan, J.Liu, Comparison of the Detection Characteristics of Trace Species using Laser-Induced Breakdown Spectroscopy and Laser Breakdown Time-of-Flight Mass Spectrometry, Sensors 15, 5982-6008, (2015).

6. G. Cristoforetti, S. Legnaioli, V. Palleschi, A. Salvetti, E. Tognoni, Appl. Phys. B 80, 559, (2005).

7. M. Capitelli, F. Capitelli and A. Eletskii, Spectrochim. Acta Part B, 55, 559–574, (2000).

8. M. Capitelli, G. Colonna, M. Catella, F. Capitelli, A. Eletskii, Chem. Phys. Lett. 316, 517, (2000).

9. E. Tognoni, G. Cristoforetti, S. Legnaioli, V. Palleschi, A. Salvetti, M. Mueller, U. Panne, I. Gornushkin, Spectrochim. Acta, Part B, 62, 1287, (2007).

10. I.R.Cristescu, I.Cristescu, L. Doerr, M. Glugla,D. Murdoch, Tritium inventories and tritium safety design principles for the fuel cycle of ITER, Nucl. Fusion, 47, S458–S463, (2007).

11. F. Rezaei, P. Karimi, S. H. Tavassoli, Effect of self-absorption correction on LIBS measurements by calibration curve and artificial neural network, Applied Physics B, 114 591–600, (2014).

12. H. E. Bauer, F. Leis and K. Niemax, Spectrochim. Acta Part B, 53, 1815–1825, (1998).

13. A. Lissovski, K. Piip, L. Hamarik, M. Aints, M. Laan, P. Paris, A. Hakola, J. Karhunen, LIBS for tungsten diagnostics in vacuum: Selection of analytes, Journal of Nuclear Materials, 463, 923–926, (2015).

14. V.I. Babushok, F.C. DeLucia Jr., J.L. Gottfried, C.A. Munson, A.W. Miziolek, Double pulse laser ablation and plasma: laser induced breakdown spectroscopy signal enhancement, Spectrochim. Acta B, 61, 999–1014, (2006).]

15. T. Donnelly, J.G. Lunney, S. Amoruso, R. Bruzzese, X. Wang, X. Ni, Double pulse ultrafast laser ablation of nickel in vacuum, J. Appl. Phys. 106, 1-5, (2009).

16. L. Mercadier, J. Hermann, C. Grisolia, A. Semerok, Plume segregation observed in hydrogen and deuterium containing plasmas produced by laser ablation of carbon fiber tiles from a fusion reactor, Spectrochim. Acta Part B, 65, 715–720, (2010).

17. G. J. van Rooij et al., Extreme hydrogen plasma densities achieved in a linear plasma generator, Appl. Phys. Lett., 90, 121501, (2007).

18. M. A. Gigosos, M. A. Gonzalez, V, Cardenoso, Spectrochimica acta B 58, 1489–1504, (2003).

19. H.Ehrich, Experimental study of Balmer-a Stark broadening, Z. Naturforsch. 34a, 188-191 (1979).

20. H. J. Kunze, Introduction to Plasma Spectroscopy, Springer, Berlin- Heidelberg, (2009).

21. H. R. Griem, Spectral Line Broadening by Plasmas, Academic Press, New York, (1974).

22. M.H.J.Hoen at al., Surface morphology and deuterium retention of tungsten after low- and high-ux deuterium plasma exposure, submitted to Nuclear Fusion, (2016).